NUKLEONIKA 2001;46(3):87–90

ORIGINAL PAPER

Monte Carlo calculations of positron implantation profiles and backscattering probabilities in gold

Asuman Aydın

Abstract The transport of charged particles through matter is worth considering for various applications. In this work, backscattering probabilities and mean penetration depths were calculated from the implantation profiles for positrons of energies 1–75 keV entering normally at various angles into a semi-infinite gold target. The theoretical results of backscattering probability and mean penetration depth are compared with other published [1, 3, 4, 10, 11, 13]. Monte Carlo calculations and experimental results for the semi-infinite gold target. In general, good agreement is observed.

Key words backscattering • computer simulation • incoming angle • mean penetration depth • positron

A. Aydın
Balıkesir University, Faculty of Science and Literature,
Department of Physics,
10100 Balıkesir, Turkey,
Tel.: +90 266/ 2493358-59 ext. 131, Fax: +90 266/ 2456366,
e-mail: aydina@balikesir.edu.tr

Received: 19 October 2000, Accepted: 12 June 2001

Introduction

Electron and positron scattering and energy loss in matter is of interest in different applications, such as studies of surfaces and solids by means of low energy electrons and positrons in electrons microscopy techniques and in medical treatment or diagnosis.

Atomic collisions of charged particles are many body problems, which can be very difficult to solve accurately. Most of the theories employ several assumptions and approximations. A good method for testing the particle transport in matter is Monte Carlo calculations.

The interactions, which positrons undergo while passing through the matter, are elastic and inelastic collisions with atoms, annihilation in flight or at rest, then slowing down and resulting in bremsstrahlung radiation. In this study, the upper limit of incident positron energy is 75 keV, therefore the contributions coming from bremsstrahlung radiation and annihilation in flight are ignored. The detailed description of the Monte Carlo code has been reported elsewhere [15, 16]. The simulation technique is based mainly on the screened Rutherford differential cross section with the spin-relativistic factor [18] and some extra total cross section information at low energies for elastic scattering. For inelastic scattering Liljequist's model [12] were used to calculate the total inelastic scattering cross section. The energy loss in the inelastic scattering process was sampled using Gryzinski's excitation function [6–8]. The detailed description of the physical ingredients involved has been reported in a number of references [15].

The program used in the study works in a wide range of energy for many metals. This program was used in our previous work [16] to calculate the transmission probabilities for gold. Now it has been modified to calculate the

backscattering probabilities and implantation profiles while keeping physical assumptions the same.

Methods of calculations

The main physical ingredients in our code are the total elastic and inelastic cross sections, the elastic differential cross section, and the energy loss distribution for the inelastic scattering. Since the detail description was given in reference [15], only the differences are highlighted here.

Elastic scattering

The screened Rutherford cross section with the spin-relativistic factor for elastic scattering [18] has been used. The spin relativistic factor K_{rel} (θ,E) is equal to the ratio of the Mott cross section to the Rutherford cross section and its value for several energies and scattering angles has been tabulated by Doggett & Spencer [5] and Idoeta & Legarda [9]. To obtain an analytic expression for K_{rel} (θ,E) as a function of the kinetic energy E of incoming positrons and the scattering angle θ, we have first determined the coefficients p_1, p_2, p_3, p_4 by fitting the expression:

$$(1a) \quad K_{rel}(\theta,E) = p_1 + p_2\theta + p_3\theta^2 + p_4\theta^3 \qquad E \text{ (MeV)}$$

for various energy values, where θ is given in radians. We have then found the energy dependence of each of the $p_i s$ in equation (1a) by fitting the expressions given below to the values $p_i s$, obtained with the angle dependence fits:

$$(1b) \quad p_1(E) = 0.998 - 0.0079E + 0.002E^2 + 0.00596E^{0.25}$$
$$(1c) \quad p_2(E) = 0.0145 + 4.144E - 0.06471E^2 - 4.448E^{0.9}$$
$$(1d) \quad p_3(E) = -0.00257 - 1.4415E + 0.147E^2 + 1.2635E^{0.9}$$
$$(1e) \quad p_4(E) = 0.0021 + 0.04576E - 0.02025E^2 - 0.0084E^{0.25}$$

where E is given in MeV.

The angular dependence of the screened Rutherford cross section is given by the factor $1/(1 - \cos\theta + 2\eta)^2$, where η is the screening angle. The screening angle η is an important parameter, affecting the shape of the angular distribution of elastically scattered positrons. The screening angle η for positrons has been calculated by Nigam and Mathur [14] using the first and second Born approximations. By assuming a suitable value of η, a reasonable angular distribution can be obtained. We have tried several energy dependent expressions for η, but the expression:

$$(2) \quad \eta = \exp(p_1 + p_2x + p_3x^2)$$

where: $x = \ln E$ (keV), $p_1 = -2.4284$, $p_2 = -0.81121$, $p_3 = -0.038521$ has given optimum results.

This expression has been obtained by taking $\eta = 0.71$ for $E = 50$ eV, and some calculated values of η using the expression obtained with the first Born approximation for $E = 10$–100 keV, and fitting a power expansion on ($\ln E$, $\ln\eta$) points.

We obtained the total elastic cross section for positrons on gold by scaling the values for phosphorus, arsenic and antimony calculated by Öztürk *et al.* [17] in the energy region 50 eV – 6 keV. We have calculated the total elastic cross section for several values of E in the range 100 keV – 1 MeV by integrating the screened Rutherford cross section with the spin relativistic factor. We have obtained the expression:

$$(3) \quad \mu_e \text{ (cm}^{-1}) = \exp(p_1 + p_2x + p_3x^2 + p_4x^3)$$

$x = \ln E$ (keV), $p_1 = 16.717$, $p_2 = -0.49848$, $p_3 = -0.056964$, $p_4 = 0.006166$ by fitting a power expansion on ($\ln E$, $\ln\mu_e$) points.

Inelastic scattering

The total inelastic scattering cross section can be calculated using the models given by Liljequist [12]. The following expression is used to fit the values calculated from Liljequist's model,

$$(4) \quad \mu_i \text{ (cm}^{-1}) = \exp(p_1 + p_2x + p_3x^2 + p_4x^3 + p_5x^4)$$

for the macroscopic total inelastic cross section, where: $x = \ln E$ (keV), $p_1 = 15.964$, $p_2 = -0.7759$, $p_3 = -0.069796$, $p_4 = 0.0217$, $p_5 = -0.0016861$ by doing a fit over ($\ln E$, $\ln\mu_i$) points.

The total ionization cross section, calculated from Gryzinski's excitation function, has been used to determine the electron shell from which the scattering occurred. Then, the energy loss in the inelastic scattering process using Gryzinski's excitation function has been sampled. The mean

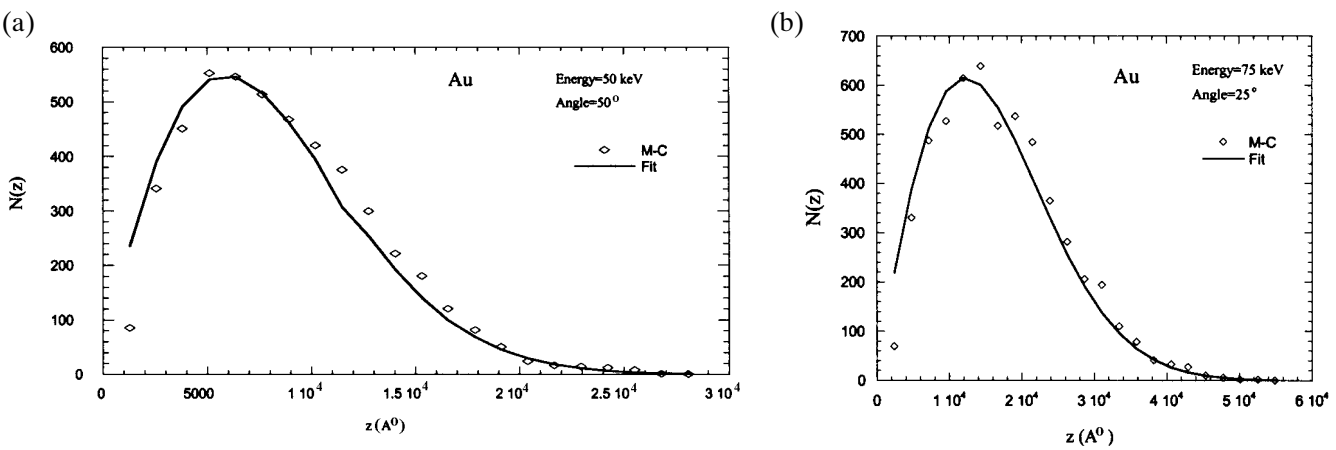

Fig. 1. Typical implantation profiles of positrons at 50 keV (at 50°) (a) and 75 keV (25°) (b) in the semi-infinite gold.

Table 1. Mean binding energies (E_b) and number of electrons (n_e) for each electron shell of the gold atom.

Z	Shell	n_e	E_b (eV)
79	.....	.....	.....
	4*s*4*p*	8	624
	4*d*	10	341
	5*s*	2	108
	4*f*5*p*	20	78
	5*d*6*s*	11	9.226

binding energies and the number of electrons in various electron shells in gold given in Table 1 were used in our calculations [12].

Results and conclusions

In our previous work, only backscattering probabilities entering normally into the semi-infinite gold and silver targets and their mean penetration depths have been considered. Details of the Monte Carlo programs, developed to obtain the positron implantation profiles in various metals were also given in that work [2]. In the present work, backscattering probabilities of positrons entering into the semi-infinite gold target at various angles (as a different point of view compared to the previous work) are studied as a function of energy. The geometrical structures used in our codes are those corresponding to a semi-infinite medium. The particle simulation is continued until a maximum number of 10^4 histories have taken place. The positrons in a semi-infinite medium have been followed until they have backscattered or slowed down below 50 eV.

Fig. 1 shows typical implantation profiles for positrons of 50 keV (at 50°) and 75 keV (at 25°) in the semi-infinite gold. The mean penetration depths <z> were calculated by fitting the implantation profiles with the distribution function suggested by Valkealahti and Nieminen [19, 20]

$$(5) \qquad P(z) = (mz^{m-1}/z_0^{m})\exp[-(z/z_0)^{m}]$$

where z is the penetration depth, and z_0 and m are parameters.

Fig. 2 shows the mean penetration depths <z> of positron entering normally into the gold target as a function of their energy. The values calculated in this study for gold are compared with those of Baker *et al.* [3], Jensen and Walker [10] and Aers [1]. As seen from Fig. 2, the mean penetration depths increase with positron energy. The results are in satisfactory agreement with other Monte Carlo results but systematically smaller than the experimental data. The discrepancy of mean penetration depths for low energies between our results and other Monte Carlo results is mainly due to the calculation techniques. Although Aers [1], and Jensen and Walker [10] used the Penn dielectric loss function or the Lindhard dielectric function to model inelastic scattering and elastic scattering cross sections obtained from a partial wave function, we used different calculation technique as discussed in the text.

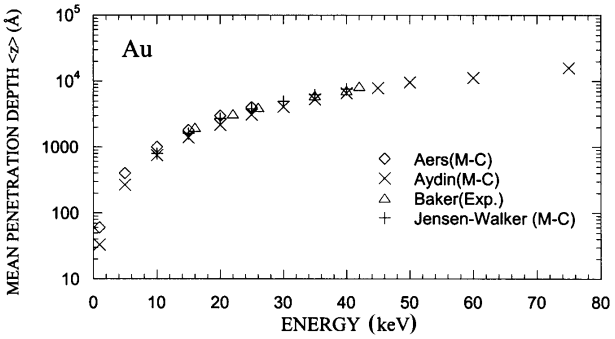

Fig. 2. Mean penetration depth <z> entering normally into the gold target as a function of positron energy.

Fig. 3 shows the calculated backscattering probabilities for positrons entering normally into the semi infinite gold target as a function of energy in comparison with experimental results reported by Coleman *et al.* [4], Mäkinen *et al.* [13] as well as with other Monte Carlo data given by Jensen *et al.* [11], Jensen and Walker [10]. The calculated backscattering probabilities are in good agreement with other experimental and theoretical results. Fig. 4 shows the calculated backscattering probabilities for positrons entering into the semi-infinite gold target at various angles in the energy range 1–75 keV. As seen from Fig. 4 the backscattering probabilities increase with increasing incoming positron energies and incident angle. For instance, backscattering probabilities of positron entering into the semi-infinite gold target are 0.270 and 0.560 for 1 keV positron energy at incident angles of 25° and 75° in relation to the surface, respectively. For 75 keV positron energy, these probabilities are calculated as 0.428 and 0.699 at the same incident angles, 25° and 75°, respectively. In this work, a detail comparison of our results with the literature cannot be made due to the lack of data on calculations and measurements of backscattering probabilities of positrons at various angles and mean penetration depths for the semi-infinite gold target.

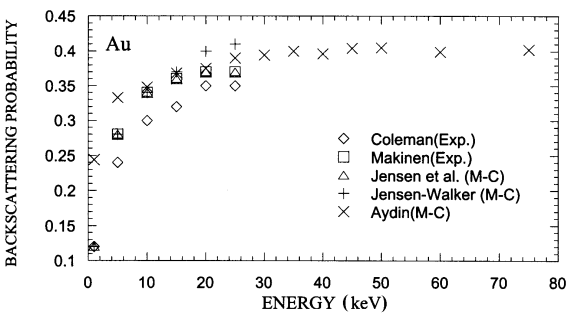

Fig. 3. Comparison of backscattering probabilities of positrons in the gold target.

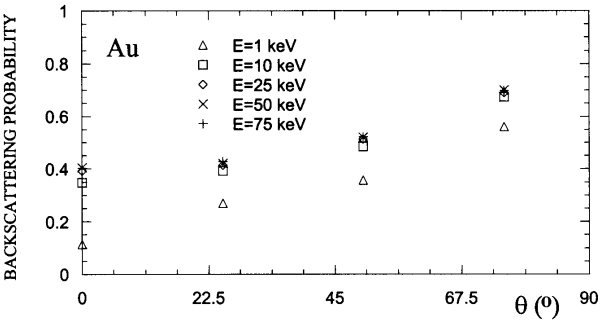

Fig. 4. Backscattering probabilities as a function of positron incoming angles.

References

1. Aers GC (1994) Positron stopping profiles in multilayered systems. J Appl Phys 76;3:1622–1632
2. Aydın A (2000) Monte Carlo calculations of positron implantation profiles in silver and gold. Radiat Phys Chem 59;3:277–280
3. Baker AJ, Chilton NB, Jensen KO, Walker AB, Coleman PG (1991) Material dependence of positron implantation depth. Appl Phys Lett 59;23:2962–2964
4. Coleman PG, Albrech L, Jensen KO, Walker AB (1992) Positron backscattering from elemental solids. J Phys Condens Mat 4:10311–10322
5. Doggett JA, Spencer LV (1956) Elastic scattering of electrons and positrons by point nuclei. Phys Rev 103;6:1597–1601
6. Gryzinski M (1965) Classical theory of atomic collisions. I. Theory of inelastic collisions. Phys Rev A 138:336–358
7. Gryzinski M (1965) Two-particle collisions. I. General relations for collisions in the laboratory system. Phys Rev A 138:305–321
8. Gryzinski M (1965) Two-particle collisions. II. Coulomb collisions in the laboratory system of co-ordinates. Phys Rev A 138:322–335
9. Idoeta R, Legarda F (1992) Review and calculation of Mott scattering cross section by unscreened point nuclei. Nucl Instrum Meth B 71:116–125
10. Jensen KO, Walker AB (1993) Monte Carlo simulation of the transport of fast electrons and positrons in solids. Surf Sci 292:83–97
11. Jensen, KO, Walker AB, Bouarissa N (1991) Monte Carlo simulation of positron slowing down in aluminium. In: Schultz PJ, Massoumi GR, Simpson PJ (eds) Positron beams for solids and surfaces. AIP Conf Proc. American Institute of Physics, New York, vol. 218, pp 19–28
12. Liljequist D (1983) A simple calculation of inelastic mean free path and stopping power for 50 eV–50 keV electrons in solids. J Phys D: Appl Phys 16:1567–1582
13. Mäkinen J, Palko S, Martikainen J, Hautojärvi P (1992) Positron backscaterring probabilities from solid surfaces at 2–30 keV. J Phys Condens Mat 4:L503-L508
14. Nigam BP, Mathur VS (1961) Difference in the multiple scattering of electrons and positrons. Phys Rev 121;6:1577–1580
15. Özmutlu EN, Aydın A (1994) Monte Carlo calculations of 50 eV – 1 MeV positrons in aluminum. Appl Radiat Isot 45;9:963–971
16. Özmutlu EN, Aydın A (1997) Monte Carlo calculations of medium energy positrons in metals. Appl Radiat Isot 48;3:403–406
17. Öztürk N, Williamson W Jr, Antolak AJ (1992) Elastic scattering of electrons and positrons by bound phosphorus, indium and antimony atoms. J Appl Phys 71;1:11–14
18. Seltzer SM (1991) Electron-Photon Monte-Carlo calculations: The ETRAN code. Appl Radiat Isot 42:917–941
19. Valkealahti S, Nieminen RM (1983a) Monte Carlo calculations of keV electron and positron slowing down in solids. Appl Phys A 32:95–106
20. Valkealahti S, Nieminen, RM (1984b) Monte Carlo calculations of keV electron and positron slowing down in solids. II. Appl Phys A 35:51–59